

North Equatorial Current and Kuroshio Velocity Variations Affect Body Length and Distribution of the Japanese eel *Anguilla japonica* in Taiwan and Japan

Yi-Chun Kuo

National Taiwan University

Kuan-Mei Hsiung

National Taiwan University

Yen-Ting Lin

National Taiwan University

Yu-Heng Tseng (✉ tsengyh@ntu.edu.tw)

National Taiwan University

Yu-San Han

National Taiwan University

Research Article

Keywords: Arrival wave, Larval duration, Larval dispersal, Total length

Posted Date: October 20th, 2021

DOI: <https://doi.org/10.21203/rs.3.rs-964045/v1>

License:   This work is licensed under a Creative Commons Attribution 4.0 International License.

[Read Full License](#)

Abstract

The larval stage of Japanese eel travels a substantial distance over a long duration through the North Equatorial Current (NEC) and the Kuroshio, and the spawning behavior of mature eels leads to monthly arrival waves in eastern Taiwan between November and February. The total length (TL) of the glass eel relates to its larval duration and age; therefore, the TL can indicate the larval duration. The monthly mean TLs of eels along eastern Taiwan from 2010–2021 were used to estimate the batch age, and the recruitment patterns and relative abundances were compared. The TLs of glass eels followed a normal distribution, and the estimated ages were highly correlated with their mean TLs. Early recruit TLs were significantly greater than those of late recruits. The mean tracer drift time was longer in early recruitment months (November–December) than in later dates (February–March). The recruitment lag was approximately 1–1.5 months, with relative recruitment higher in the early recruitment months than in later months. Cohorts followed the main streams of the NEC and Kuroshio, and the monthly velocity changes of these currents could affect the TLs as well as the distribution patterns of Japanese glass eels in Taiwan and Japan.

Introduction

The Japanese eel *Anguilla japonica* Temminck and Schlegel 1847 is a temperate catadromous fish with a complex life history that is mainly distributed in Taiwan, China, Korea, and Japan^{1–5}. Although it is a commercially valuable aquaculture species in East Asia, large-scale commercial artificial propagation is currently not possible, and the fry used in aquaculture can only be obtained by capture in estuarine and coastal waters during their upstream migration. Japanese eel resources have been declining significantly since the late 1970s^{6–8}, and the annual catch of adult wild Japanese eels in Japan has decreased from approximately 3,000 tons in the 1970s to less than 80 tons in recent years (Annual Report of the Ministry of Agriculture, Forestry and Fisheries, Japan, https://www.maff.go.jp/j/tokei/kouhyou/naisui_gyosei/index.html). In response to this resource crisis, the Japanese eel was listed as an “endangered” species in 2013 by the Ministry of the Environment, Government of Japan. In 2014, it was included in the IUCN Red List of Threatened Species as an endangered species^{9,10}, and in 2017, it was deemed “critically endangered” in the freshwater Red List by the Forest Bureau of the Council of Agriculture, Taiwan. A combination of factors has caused this decline, including habitat degradation, overfishing, and fluctuations in oceanic conditions^{8,11}. To ensure the resource sustainability of the Japanese eel, a better understanding of its life history is necessary.

Mature eels spawn in the western waters of the West Mariana Ridge located at 12.5–16° N, 141–142° E within the North Equatorial Current (NEC)^{2,3,12} mainly between May and September^{5,7,13,14}. The spawning event occurs at a depth of approximately 160–250 m¹⁵. After hatching, the *A. japonica* larvae (leptocephali) have a limited swimming speed, while the current velocity of the surrounding NEC water is much greater (typical zonal velocity 30 cm/s)¹⁶. Thus, the larvae drift passively by way of oceanic currents for long-distance dispersal. In addition, as the larvae drift with the current, they remain in the

upper surface waters (approximately 30–50 m deep) during the daytime, and dive into deeper waters (approximately 70–100 m deep) at night¹⁷, which is an important behavioral trait known as diel vertical migration (DVM). The NEC bifurcates at its westernmost boundary off the coast of the Philippines into the north-flowing Kuroshio and south-flowing Mindanao currents, a feature known as the NEC bifurcation¹⁸. *A. japonica* larvae must enter the Kuroshio in the bifurcation zone to reach their habitats in East Asian countries¹². The leptocephali metamorphose into juvenile eels (glass eels) after 4–6 months of drifting^{2,3,19,20}. Metamorphosing larvae (52.7–61.2 mm) were collected only in the area to the east of Taiwan (21–26 °N, 121–129 °E), while glass eels (51.3–61.2 mm) were found only within or west of the Kuroshio¹². These distributions suggest that leptocephali begin to metamorphose within or just east of the Kuroshio. After completion of metamorphosis, the glass eels adopt a benthic sheltering behavior to escape the oceanic current and actively swim toward nearby estuaries and rivers for growth¹. Generally, the early life stages of *A. japonica* in the ocean are the most vulnerable periods. Biological and physical changes in the oceanic environment may significantly influence their transport processes, mortality, growth rates, and recruitment dynamics^{11,21,22}.

Tsukamoto et al. (2003) analyzed the otolith microstructure of *A. japonica* leptocephali collected near the spawning area in July 1991 and estimated their ages to determine spawning times. These leptocephali had a total length of 10–30 mm and consisted of two batches of individuals hatched during the new moon periods of May and June. The “New Moon Hypothesis,” was proposed to explain the timing of eel spawning⁴. This hypothesis assumes that the abundance of recruited glass eels along their transport route should be uneven and may exhibit batch-like cohorts. Among East Asian countries, Taiwan is closest to the spawning ground of the Japanese eel, and it is the first country to capture this species (Fig. 1). Batch-like waves were indeed found in the waters of eastern Taiwan, where the main stream of the Kuroshio flows along its east coast. The arrival waves have a periodicity of approximately one month, which coincides with their monthly spawning behavior²⁰.

In a previous study, the *A. japonica* glass eel specimens collected from Taiwan from 1984 to 2013 indicated that the mean total length (TL) and larval duration (LD) in three climates (El Niño, normal, and La Niña) were significantly different, with El Niño years having larger TLs and LDs than those of the La Niña years²³. This finding suggests that El Niño-Southern Oscillation (ENSO) events may have significant impacts on the TL and LD of the glass eel, since they are connected with NEC bifurcation^{24,25}, current transport²⁶, and current velocity²⁷. The eel spawning site and passive transport by the NEC may affect the fluctuation of TL and LD in the glass eel²³. If the eel spawns south of the salinity front of the NEC, the southward movement of the salinity front associated with the northward movement of the NEC bifurcation during El Niño years may cause the larvae to experience slower currents and broaden the distance between their spawning ground and NEC bifurcation. Thus, the time needed for eel larvae to enter the Kuroshio from their spawning grounds would be prolonged. In addition, the relationship between the mean TL and LD showed a statistically positive correlation in both the Japanese glass eel²³ and *A. marmorata*²⁸. TL could be an alternate for representing the LD measure. NEC/Kuroshio velocity variations

are monthly dependent²⁹; therefore, glass eels sampled from different months may show fluctuations of age as well as TL.

To better understand the effects of monthly dependent NEC/Kuroshio velocity variations on eel larval size in Taiwan, as well as its distribution pattern in East Asia, the TL of *A. japonica* glass eel in Taiwan and its recruitment dynamics in Taiwan and Japan were analyzed. The estimated transport time of each recruitment cohort was calculated using the glass eel arrival time and the nearest new moon period six month prior. A particle tracking simulation was used to estimate the transport patterns of the eel larvae spawned between May and September from the supposed spawning ground to Taiwan.

Materials And Methods

Glass eel collection and total length (TL) measurement

The estuaries of the Yilan and Hualien counties of eastern Taiwan were the chosen regions for monitoring the arrival of Japanese glass eels (Fig. 1). This species is easily distinguished from other eels (e.g., *A. marmorata*, *A. bicolor pacifica*, and *A. luzonensis*) by their lack of caudal cutaneous pigmentation⁷, and they are the target eel species for Taiwanese fisheries in winter. The pigmentation stage of the glass eel (V_A , V_B , VI_{A1} , VI_{A2} , VI_{A3} , VI_{A4} , and VI_B) was determined based on Tesch (2003). The main fishing season in Taiwan is from November to February. The Japanese glass eel specimens were collected at night during the fishing season using a hand-trawling net, a fyke net, or a boat net. They were collected from Yilan (24.7163 °N, 121.8348 °E) and Hualien (23.4612 °N, 121.5008 °E) in Taiwan between December 2010 and February 2021. A total of 5,595 glass eels were used to measure the TLs each month.

The Japanese glass eel samples were fixed and preserved in 95 % ethanol after collection. The samples were measured after one month when the shrinkage of the samples stopped (approximately 6 %, data not shown). Only glass eels in the pigment stages V_A and V_B , which are considered the earliest phases of glass eels arriving in estuaries¹, were selected and their TL was measured to the nearest 0.1 mm.

Eel sampling was approved by the Fishery Agency, Council of Agriculture, Executive Yuan, Taiwan. Animal use approval “NTU-108-EL-00130” was obtained from the Animal Research Committee of National Taiwan University and reviewed by the Institutional Animal Care and Use Committee (IACUC).

Glass eel catch information in Taiwan and Japan

The weekly/monthly catch data of the glass eel from 2010 through 2021 in Taiwan and Japan were collected by the Japan Aquaculture Information News (daily fax), the Taiwan Japanese Glass Eel Reporting System (Fisheries Agency, Council of Agriculture, Executive Yuan, Taiwan), and glass eel traders in Taiwan. The catch data included glass eels caught throughout Taiwan and Japan.

Estimating the mean ages of the arrival batches recruiting to eastern Taiwan

Yilan and Hualien in Taiwan are the first locations to collect glass eels in Taiwan and East Asia, and the recruited samples showed arrival waves at approximately one-month intervals²⁰. Based on the weekly data from the Taiwan Japanese Glass Eel Reporting System and the daily information from the Japan Aquaculture Information News, the first arrival time of the Japanese glass eel in Yilan usually begins in mid-November. Since the eels spawn near the new moon period, and the mean ages of the glass eels from Taiwan were approximately 6 months^{5,19,20}, the estimated spawning date of each arrival batch would have occurred during the nearest new moon approximately 6-month prior to the catch date. Thus, the estimated theoretical age of each arrival batch of the glass eel was determined based on the date of its supposed spawning new moon and the date of its arrival peak in Yilan.

Ocean circulation model of the North Pacific

We conducted a Lagrangian tracer study based on the 1/12° global HYbrid Coordinate Ocean Model (HYCOM) (GLBv0.08, https://www.hycom.org/dataserver/gofs-3_pt1/reanalysis, for 1994–2015 and GLBy0.08, https://www.hycom.org/dataserver/gofs-3_pt1/analysis, for 2016–2019). The high-resolution HYCOM provides an appropriate modeling framework to simulate ocean circulation in the North Pacific, which is useful for investigating glass eel larval migration. HYCOM data are daily assimilative global results using three types of vertical coordinates: z-level, terrain-following, and isopycnic³⁰. The model uses 32 vertical levels with a horizontal resolution of approximately 7 km. Quality controlled bathymetric data from the Naval Research Laboratory's Digital Bathymetry Data Base 2 (NRL DBDB2) were used. Surface forces, including wind stress, wind speed, heat flux, and precipitation, were retrieved from the Navy Operational Global Atmospheric Prediction System (NOGAPS).

Simulation of migration time from spawning ground to Luzon Strait

Tracer simulations were performed to study the migratory behavior of the larvae. Since the 1/12° global HYCOM reanalysis assimilated all available oceanic data, it reproduced the realistic flow patterns of the Kuroshio east of Taiwan and around the Luzon Strait³¹. An offline Lagrangian particle-tracking method was used to investigate the potential migration routes of eel larvae from the spawning area to the Luzon Strait (Fig. 1). Both ocean currents and biological swimming speeds were considered in the model. The former was extracted from the 1/12° global HYCOM climatology (1994–2019) and the latter increased linearly with age.

The representative tracer experiment was performed at a depth of 100 m from May to September, during the main spawning season of *A. japonica*, from 137–140° E and 12–16° N. The overall mean tracer drift time from the presumed spawning site to the Luzon Strait between 1994 and 2020 was calculated. A total of 10,000 particles (0.5° × 0.5°) were set to drift passively in the first 10 days (simulating the larval

stage), and were released on May 1st, June 1st, July 1st and August 1st /September 1st, and swam actively afterward.

The horizontal swimming direction of the eel larvae was calculated using Equation (1).

$$u_s = V \cdot \frac{u_c}{\sqrt{u_c^2 + v_c^2}}, v_s = V \cdot \frac{v_c}{\sqrt{u_c^2 + v_c^2}} \quad (1)$$

Here, u_s and v_s represent the x and y components of the particle swimming velocity with the current, respectively. V is the eel larval swimming speed, and u_c and v_c are the x and y components of the current velocity, respectively. After hatching, the particles had a velocity of 1.5 cm/s from the 11th day and increased their speed by 1.5 cm/s per month up to 6 cm/s. The speed was maintained at 6 cm/s until the end of the simulation. A similar procedure was applied by Rypina et al. (2014) and Chang et al. (2015) to estimate the migration of American eels from the Sargasso Sea and Japanese eels from their spawning site in the Western Pacific Ocean. Only the particles with migration routes into the Kuroshio zone (18–20° N, 121–124° E) were considered effective, and those remaining in the western North Pacific Ocean, those entering the Mindanao Current, and those reaching the Kuroshio after 180 days were excluded. Therefore, only the particles entering into the Kuroshio zone within 180 days, which was the expected average age of the juvenile eels when they successfully migrated were considered.

Data analysis

Differences in the total length (mean \pm SD) between monthly samples were tested using a one-way analysis of variance (ANOVA) followed by Tukey's honestly significant difference (HSD) multiple-comparison test. The data of recruitment percentage of Taiwan among months did not pass the normal distribution test; thus, nonparametric statistics of the Mann-Whitney test were performed to compare differences in the recruitment percentage of Taiwan among months. Linear regression was used to analyze the relationship between the total length and the estimated age of the glass eels. SPSS (Statistical Package for the Social Science) software (version 16.0) was used for the statistical analysis. Differences were considered significant at $P < 0.05$.

Results

Glass eel TL

The Japanese glass eel specimens analyzed in this study were collected in the estuaries of Yilan and Hualien from November 2010 to February 2021. A previous study indicated that the mean TLs of the older stage (V_{IA}) glass eels were significantly less than those of the younger stages (V_A and V_B)³⁴. Older eels may stay longer in estuaries, and their growth may be markedly affected by the estuarine environment. Thus, only the specimens of stage V_A and stage V_B were used in this study for consistency. A total of 5,595 specimens of the Japanese glass eel were collected, and their TL was measured. The TL

frequency distribution ranged from 52 to 62 mm with an interval of 1 mm, forming a normal distribution with an average TL of 56.9 mm (Fig. 2).

The correlation of TL and estimated age of glass eels in eastern Taiwan

In this study, the theoretical age of Japanese glass eels for each arrival batch was estimated based on the time differences between the new moon of the presumptive spawning time and the peak catch time of each glass eel wave in the Yilan estuary, based on data from the Taiwan Japanese Glass Eel Reporting System and the daily fax from the Japan Aquaculture Information News. The arrival waves in Taiwan were found between November and March, corresponding to their spawning times between May and September, with most waves occurring in December and January, corresponding to their spawning times in June and July. For each arrival batch, at least 50 individuals were randomly chosen and their TLs were measured. The estimated age of each arrival wave in Yilan, Taiwan, were significantly positively correlated with their mean TLs ($R^2 = 0.31$, $p = 0.002$) (Fig. 3).

The mean TLs of specimens in each month in eastern Taiwan

The mean TLs of the specimens from each month (November to February/March) in eastern Taiwan were: November – 57.2 ± 2.1 mm (s.d.), $n = 1818$; December – 57.0 ± 2.4 mm (s.d.), $n = 1610$; January – 56.6 ± 2.3 mm (s.d.), $n = 1626$; and February/March – 56.3 ± 2.1 mm (s.d.), $n = 541$ (Fig. 4). The mean TLs of Japanese glass eels decreased monthly with significance, with the largest mean TLs in November and December ($p = 0.198$) (early recruits) and lowest mean TLs in February and March ($p = 0.025$) (late recruits).

NEC/Kuroshio long-term monthly velocity

The Kuroshio is the main western boundary current in the North Pacific, and the NEC is its upstream source. The westward flow speed of the NEC gradually increases toward the main stream. The NEC bifurcates before reaching the coast of the Philippines, while the northern branch develops into the Kuroshio. The northward Kuroshio is enhanced to the east of the Philippines and develops more baroclinity. Both the NEC and Kuroshio exhibit strong seasonal variability with clear monthly-dependent changes^{33,34}. The surface climatological NEC bifurcation latitude is approximately 12.7° N based on 40 years of Simple Ocean Data Assimilation (SODA) reanalysis³⁵. The bifurcation latitude moves toward the north with depth owing to the baroclinity of the NEC. The climatological mean of the subsurface (96 m) NEC bifurcation latitude was estimated to be approximately 13.6° N by Meng et al (2011), which is similar to the estimation of 14° N using the 26-yr HYCOM reanalysis in this study. The seasonal variability of the bifurcation latitude is significant, reaching the southernmost latitude in May–June, and then moving northward until fall (October–November)^{25,36,37}. The NEC main stream migrates meridionally along with the NEC bifurcation latitude. However, different segments of the NEC do not move simultaneously; hence, the time-space variations are more complex. Fig. 5a shows the modeled monthly variation of the main

stream speed between 13° N and 14° N at 100 m depth, corresponding to the south of the NEC bifurcation. Between 135° E and 140° E, the monthly change in the main stream speed is unclear. To the west of 135° E, there is a decreasing trend from early summer (May to June) to winter (November to December). This is related to the seasonal movement of NEC bifurcation. From summer to autumn, the NEC bifurcation moves northward; therefore, the flow speed in Fig. 5a decreases with time as the NEC main stream center (maxima) moves northward, away from the region at 13° N –14° N. Fig. 5b shows the monthly variation of the main stream speed between 15° N and 16° N, corresponding to area north of the NEC bifurcation. The main stream speed changes in Fig. 5b show the opposite trend of the monthly variation compared to those in Fig. 5a. As the NEC moves northward after May, its main stream center moves closer to the north of the bifurcation (15° N–16° N), and the flow speed between 15° N and 16° N increases correspondingly. Fig. 5c shows the monthly variation of the northward Kuroshio (120° E–125° E). From October to April, the current speed between 15.5° N and 19.5° N consistently increases as the NEC bifurcation moves southward. This can accelerate the reach of the Japanese eel to the western North Pacific. To the south of 15° N, a seasonal trend was absent.

Numerical simulation of larval transport

Several representative tracer simulation experiments further confirmed that the tracers (larvae) drifted along the main stream of the westward-flowing NEC and reached the east coast of the Philippines three to four months later. They then flowed along the northward Kuroshio and finally approached the south of Taiwan (Fig. 1). The modeled mean tracer drift time during 1994–2019 from the spawning site to the south of Taiwan is presented in Fig. 6. The tracers were released at the beginning of May, June, July, and August/September. The particles released from May 1st required the longest drifting time (173.5 ± 34.6 d), followed by June 1 (166.7 ± 24.2 d), July 1 (161.8 ± 24.2 d), and August 1st /September 1st (160.4 ± 24.2 d) (Fig. 6). The actual drifting days from the spawning area are shaded in Fig. 6. These results are consistent with the monthly flow speed variations shown in Fig. 5. To the north of the NEC bifurcation, at approximately 14° N, the main stream speed increases from early summer to autumn, while the Kuroshio near the Philippine coast further strengthens after autumn. When the particles were released in May, they reached the south of Taiwan (Luzon Strait) between October and December. When the particles were released in August or September, they reach south of Taiwan in a shorter time.

The monthly catch percentage of the glass eel in Taiwan and Japan

The recruitment of the Japanese glass eel was mainly between November and February in Taiwan, with an arrival peak in or near December (Fig. 7). There were very few recruits in March in Taiwan. In contrast, the recruitment of the Japanese glass eel usually began in December and ended in late April in Japan, with an arrival peak in or near February (Fig. 7). The recruitment lag between Taiwan and Japan was approximately 1–1.5 months.

The monthly recruitment proportion between Taiwan and Japan

The monthly catch data of the Japanese glass eels in Taiwan and Japan between 2010 and 2021 are shown in Supplementary Table S1. Since the movement of recruitment waves of the Japanese glass eel from Taiwan to Japan requires approximately 1–1.5 months, the glass eels caught in November in Taiwan and December in Japan were mainly from the same cohorts. Thus, they were used to calculate the relative proportion of glass eel recruitment in Taiwan for each month. The results indicate that the relative percentage of glass eels in Taiwan was significantly elevated in early recruitment months (November–January), then decreased in late recruitment months (February–March) ($p = 0.693$ in 11/2 and 12/1, $p = 0.393$ in 12/1 and 1/2; $p = 0.023$ in 1/2 and 2/3; $p < 0.001$ in 2/3 and 3/4; $p < 0.001$ in 3/4 and 11/12) (Fig. 8).

Discussion

The overall TLs of Japanese glass eels in Yilan, Taiwan, ranged from 52 to 62 mm, forming a normal distribution with an average length of 56.9 mm (Fig. 2). However, the mean TLs of each batch ranged from 54.6 to 59.9 mm. Based on otolith measurements, it has been suggested that the total length of the Japanese glass eel is highly correlated with age^{23,38,39}. In this study, the estimated age of each arrival wave in Yilan was found to positively correlate with the mean TL (Fig. 3), supporting the relationship between age and TL of the glass eel. The varied mean TL of each arrival batch in Taiwan suggested that each wave possessed a different mean transport time. Variations in mean ages between arrival waves may reflect differentiations in the current speed during larval transport from the spawning site to Taiwan. Alternatively, these batches of glass eels may spawn at different sites in the range of 12–16° N during the new moon period, and then drift along different routes on the NEC and Kuroshio to the Yilan offshore area. Han et al. (2016) found that each batch of glass eels caught offshore in December of three consecutive year classes at Yilan, had a narrow range of ages between years. This implies that most individuals in the arrival peaks spawn in the same month and thus belong to the same cohort. Furthermore, tracer simulation also supported that each batch of glass eels takes approximately 160–170 days to reach the Luzon Strait from their spawning site (Fig. 6). All of this data suggests that the potential mixing of glass eels between monthly spawning cohorts was low, at least in Taiwan.

One of the main dispersal routes of Japanese eel larvae is from Taiwan to Japan by the Kuroshio stream. It is estimated that the time needed for the larval eels to travel from Taiwan to Kyushu, Japan (approximately 1,000 km) is 25.3 ± 6.4 days¹⁴. The mean velocity of the Kuroshio along the Pacific coast of Japan is approximately 0.7–1.4 m/s^{40,41}; thus, it takes 8–16 days for the eel larvae to be transported from western to eastern Japan (approximately 1,000 km). This means that the recruitment time lag between Taiwan and Japan is expected to be close to one month, and the mean TLs of the glass eels in Japan should be greater than those in Taiwan because of their increased mean ages. The mean TLs of the glass eels in Japan ranged between 57.9 and 60.1 mm⁴², which is greater than that of the glass eel in Taiwan (56.9 mm). In addition, the recruitment of the Japanese glass eel usually started in November in Taiwan and December in Japan, and the arrival peak of the Japanese glass eel was December/January in Taiwan and January/February in Japan (Fig. 7) coinciding with a lag of approximately one month.

Since the estimated age of the glass eel was positively correlated with its TL (Fig. 3), the mean TLs of the glass eels in Japan are expected to be larger than those of glass eels in Taiwan. According to an eel trader, the Japanese glass eels from Chiba, Japan, which is the easternmost part of the Kuroshio and the farthest from the spawning site, usually have the largest TLs.

Japanese eels spawn in restricted areas (12–16° N and 141–142° E) during a specific time span (May through September)^{14,39}. The larvae are passively transported via the NEC to the east Philippines for 3-4 months and then enter the Kuroshio and move toward their habitats in East Asia. For the glass eels that arrived in Taiwan, the dispersal distance was longer in the NEC (approximately 2,500 km) than in the Kuroshio (closer to 1,000 km), and the mean NEC velocity was generally low compared to that of the Kuroshio (Fig. 5). However, the monthly velocity variations of the NEC were low compared with those of the Kuroshio (Fig. 5). A previous study has also demonstrated that recruitment dynamics and distribution of Japanese glass eels might change with global warming, due to changes in the velocity, structure, and location of the NEC, NEC bifurcation, and Kuroshio with warming climate⁴³. This suggests that the transport time the glass eels need to reach the Luzon Strait from the spawning site is significantly impacted by both the NEC and the Kuroshio. Eel larvae that spawn between May and June (early recruits) require a longer transport time (167–174 days) than those spawning between August and September (late recruits, 160 days) (Fig. 6). Therefore, a greater percentage of early recruits may metamorphose in the southern areas of East Asia due to their slower dispersal. By contrast, more late recruit eel larvae may metamorphose in the northern areas of East Asia due to their faster transport. Indeed, the relative abundance of glass eels near Taiwan relative to Japan was significantly higher in earlier recruitment months (November–December), and significantly lower during later recruitment months (February–March) (Fig. 8). Seasonal variations in the location of the NEC bifurcation can be entertained as one of the most important factors, since it is located at its southernmost latitude in May, and moves northward after that, reaching its northernmost point in September. In other words, the distance between the NEC bifurcation and Kuroshio might be wider when the NEC bifurcation is in the southern region of its range, thereby causing a longer duration of drift among the earlier recruitment cohort. In March, Japanese glass eels were scarce in Taiwan; however, they were abundant in Japan in April. This supports the concept that late recruits, which were transported with faster oceanic current velocity, would bypass Taiwan and metamorphose mainly downstream of the Kuroshio and then continue on to Japan.

Although the mean TLs of Japanese glass eels in Taiwan decreased monthly with significance, the mean TLs of each batch ranged between 54.6 and 59.9 mm with high variation. Multiple biotic/abiotic factors must be involved in this TL variation. In a previous study, it was found that ENSO events had a substantial impact on the TL of glass eels in Taiwan²³. The TLs of Japanese glass eels were significantly greater during El Niño years and less during La Niña years. The northward shifts in the NEC bifurcation and the southward shift of the salinity front during the El Niño years might have led to larvae encountering slower currents and broadening the distance between the spawning site (south of the salinity front) and the NEC bifurcation^{13,44,45}, thereby extending the journey time required for the larvae to

enter the Kuroshio from their spawning grounds²³. Since ENSO events occur periodically, the effect of ENSO on the transport time of eel larvae in each month would be offset over the long term.

It has been suggested that local eddy currents along the transport route may trap some leptocephali and result in a small amount of mixing between monthly cohorts³³. Chang et al. (2018) indicated that v-larvae may be able to remain in eddies passively (physical trapping) due to mesoscale eddy nonlinearity, and/or actively (biological attraction) due to rich food supplies in those eddies. In addition, otolith analysis indicated that Japanese eels may have a recruitment route through the mesoscale eddies to the east of Taiwan, in addition to the direct transfer route from the NEC to the Kuroshio⁴². However, based on the present study, the transport of each eel recruitment batch was generally stable in Taiwan, suggesting that the simultaneously spawning eel cohort usually forms a group and moves together. The eel larvae transported by eddies, if present, may mainly merge downstream of the Kuroshio, thus reducing the mixing degree between monthly cohorts in Taiwan. In either situation, direct observational fish larvae data from the open ocean in mesoscale eddies is necessary to evaluate their true degree of contribution to eel larvae dispersal.

Conclusion

Among the East Asian countries, Taiwan is nearest to the spawning ground of the Japanese eel, and is the first place to catch the recruited glass eels up to one month earlier than in Japan and China^{5,7,14}. The glass eels recruited to Taiwan had the lowest mean larval duration and age when compared with those from other sites¹⁴. Therefore, the dynamics of the glass eel arrival in Taiwan may serve as a useful indicator of recruitment patterns in other countries⁷. The monthly changes in the NEC and Kuroshio velocity may play an important role in affecting the TL as well as the distribution of the Japanese glass eel, by causing more abundance in Taiwan for the early recruits and in Japan for the late recruits.

Declarations

Data Availability

The datasets generated during and/or analysed during the current study are available from the corresponding author on reasonable request.

Acknowledgements

The authors thank the Ministry of Science and Technology, Executive Yuan, Taiwan (MOST 106-2313-B-002-036-MY3; MOST 109-2313-B-002-001-MY2), the Council of Agriculture, Executive Yuan, Taiwan (110-FRM-2.17-G-03), and Shanghai Jiao Tong University, China (AF4400003) for funding this project.

Authors' contributions

YCK and YHT provided numerical models, participated in the interpretation and analyses of data, and wrote the manuscript. KMH and YTL helped collect and measure the glass eel samples and provided data analysis. YSH and KMH participated in the design of the study, analyzed and interpreted the data, and wrote the manuscript. All authors read and approved the final manuscript.

Competing interests

The authors declare that they have no competing interests.

References

1. Tsukamoto, K., Umezawa, A. & Ozawa, T. Age and Growth of *Anguilla japonica* Leptocephali Collected in Western North Pacific in July 1990., **58**, 457459 (1992).
2. Tsukamoto, K. Oceanic biology: spawning of eels near a seamount. *Nature*, **439**, 929 (2006).
3. Tsukamoto, K. *et al.* Oceanic spawning ecology of freshwater eels in the western North Pacific. *Nat. Commun*, **2**, 179 (2011).
4. Han, Y. S. Temperature-dependent recruitment delay of the Japanese glass eel *Anguilla japonica* in East Asia. *Mar. Biol*, **158**, 2349–2358 (2011).
5. Dekker, W. Slipping through our hands: population dynamics of the European eel(Universiteit van Amsterdam, 2004).
6. Han, Y. S., Zhang, H., Tseng, Y. H. & Shen, M. L. Larval Japanese eel (*Anguilla japonica*) as sub surface current bio tracers on the East Asia continental shelf. *Fish. Oceanogr*, **21**, 281290 (2012).
7. Chen, J. Z., Huang, S. L. & Han, Y. S. Impact of long-term habitat loss on the Japanese eel *Anguilla japonica*. *Estuar. Coast. Shelf Sci*, **151**, 361–369 (2014).
8. Jacoby, D. & Gollock, M. *Anguilla anguilla*. The IUCN red list of threatened species. Version 2014.2(2014).
9. Jacoby, D. M. P. *et al.* Synergistic patterns of threat and the challenges facing global anguillid eel conservation. *Glob. Ecol. Conserv*, **4**, 321–333 (2015).
10. Kimura, S., Tsukamoto, K. & Sugimoto, T. A model for the larval migration of the Japanese eel: roles of the trade winds and salinity front. *Mar. Biol*, **119**, 185190 (1994).
11. Shinoda, A. *et al.* Evaluation of the larval distribution and migration of the Japanese eel in the western North Pacific. *Rev. Fish Biol. Fish*, **21**, 591611 (2011).
12. Zenimoto, K. *et al.* The effects of seasonal and interannual variability of oceanic structure in the western Pacific North Equatorial Current on larval transport of the Japanese eel *Anguilla japonica*. *J. Fish Biol*, **74**, 18781890 (2009).

13. Han, Y. S. *et al.* Dispersal characteristics and pathways of Japanese glass eel in the East Asian Continental Shelf. *Sustain*, **11**, 1–18 (2019).
14. Aoyama, J. *et al.* Spawning sites of the Japanese eel in relation to oceanographic structure and the West Mariana Ridge. *PLoS One*, **9**, e88759 (2014).
15. Zhang, L. *et al.* Structure and variability of the North Equatorial Current/Undercurrent from mooring measurements at 130° E in the Western Pacific. *Sci. Rep*, **7**, 1–9 (2017).
16. Otake, T., Inagaki, T., Hasumoto, H., Mochioka, N. & Tsukamoto, K. Diel vertical distribution of *Anguilla japonica leptocephali*. *Ichthyol. Res*, **45**, 208211 (1998).
17. Toole, J. M., Millard, R. C., Wang, Z. & Pu, S. Observations of the Pacific North Equatorial Current bifurcation at the Philippine coast. *J. Phys. Oceanogr*, **20**, 307318 (1990).
18. Cheng, P. W. & Tzeng, W. N. Timing of metamorphosis and estuarine arrival across the dispersal range of the Japanese eel *Anguilla japonica*. *Mar. Ecol. Prog. Ser*, **131**, 87–96 (1996).
19. Han, Y. S., Wu, C. R. & Iizuka, Y. Batch-like arrival waves of glass eels of *Anguilla japonica* in offshore waters of Taiwan. *Zool. Stud*, **55**, (2016).
20. Chang, Y. L., Sheng, J., Ohashi, K., Béguer Pon, M. & Miyazawa, Y. Impacts of interannual ocean circulation variability on Japanese eel larval migration in the western North Pacific Ocean. *PLoS One*, **10**, e0144423 (2015).
21. Houde, E. D. Emerging from Hjort's shadow. *J. Northwest Atl. Fish. Sci*, **41**, 53–70 (2008).
22. Hsiung, K. M., Kimura, S., Han, Y. S., Takeshige, A. & Iizuka, Y. Effect of ENSO events on larval and juvenile duration and transport of Japanese eel (*Anguilla japonica*). *PLoS One*, **13**, e0195544 (2018).
23. Qiu, B. & Lukas, R. Seasonal and interannual variability of the North Equatorial Current, the Mindanao Current, and the Kuroshio along the Pacific western boundary. *J. Geophys. Res. Ocean*, **101**, 1231512330 (1996).
24. Qiu, B. & Chen, S. Interannual to decadal variability in the bifurcation of the North Equatorial Current off the Philippines. *J. Phys. Oceanogr*, **40**, 25252538 (2010).
25. Hu, S. & Hu, D. Variability of the Pacific North Equatorial Current from repeated shipboard acoustic Doppler current profiler measurements. *J. Oceanogr*, **70**, 559–571 (2014).
26. Hsu, A. C., Xue, H., Chai, F., Xiu, P. & Han, Y. S. Variability of the Pacific North Equatorial Current and its implications on Japanese eel (*Anguilla japonica*) larval migration. *Fish. Oceanogr*, **26**, 251267 (2017).
27. KURoki, M. *et al.* Correspondence between otolith microstructural changes and early life history events in *Anguilla marmorata leptocephali* and glass eels. *Coast Mar Sci*, **29**, 154–161 (2005).
28. Qiu, B. *et al.* The Pacific north equatorial current: new insights from the origins of the Kuroshio and Mindanao currents (OKMC) project. *Oceanography*, **28**, 24–33 (2015).
29. Bleck, R. An oceanic general circulation model framed in hybrid isopycnic-Cartesian coordinates. *Ocean Model*, **4**, 55–88 (2002).

30. Chen, Y., Zhai, F. & Li, P. Decadal variation of the Kuroshio intrusion into the South China Sea during 1992–2016. *J. Geophys. Res. Ocean.* **125**, (2020).
31. Rypina, I. I., Llopiz, J. K., Pratt, L. J. & Lozier, M. S. Dispersal pathways of American eel larvae from the Sargasso Sea. *Limnol. Oceanogr.* **59**, 1704–1714 (2014).
32. Tseng, Y. H., Shen, M. L., Jan, S., Dietrich, D. E. & Chiang, C. P. Validation of the Kuroshio current system in the dual-domain Pacific Ocean model framework. *Prog. Oceanogr.* **105**, 102–124 (2012).
33. Liu, X. & Zhou, H. Seasonal variations of the North Equatorial Current across the Pacific Ocean. *J. Geophys. Res. Ocean.* **125**, e2019JC015895 (2020).
34. Meng, Q., Wang, F. & Liu, N. Low-frequency variability of the North Equatorial Current bifurcation in the past 40 years from SODA. *Acta Oceanol. Sin.* **30**, 14 (2011).
35. Chen, Z. & Wu, L. Dynamics of the seasonal variation of the North Equatorial Current bifurcation. *J. Geophys. Res. Ocean.* **116**, (2011).
36. Wang, Q. & Hu, D. Bifurcation of the North Equatorial Current derived from altimetry in the Pacific Ocean. *J. Hydrodyn. Ser. B*, **18**, 620–626 (2006).
37. Tsukamoto, K. Discovery of the spawning area for Japanese eel. *Nature*, **356**, 789791 (1992).
38. Ishikawa, S. *et al.* Spawning time and place of the Japanese eel *Anguilla japonica* in the North Equatorial Current of the western North Pacific Ocean. *Fish. Sci.* **67**, 10971103 (2001).
39. Yang, Y., Liu, C. T., Hu, J. H. & Koga, M. Taiwan Current (Kuroshio) and impinging eddies. *J. Oceanogr.* **55**, 609–617 (1999).
40. Jan, S. *et al.* Large variability of the Kuroshio at 23.75 N east of Taiwan. *J. Geophys. Res. Ocean.* **120**, 1825–1840 (2015).
41. Fukuda, N. *et al.* Location, size and age at onset of metamorphosis in the Japanese eel *Anguilla japonica*. *J. Fish Biol.* **92**, 1342–1358 (2018).
42. Hsiung, K. & Kimura, S. Deep-Sea Research Part II Impacts of global warming on larval and juvenile transport of Japanese eels (*Anguilla japonica*). 1–11 (2019)
doi:<https://doi.org/10.1016/j.dsr2.2019.104685>.
43. Kim, H. *et al.* Effect of El Niño on migration and larval transport of the Japanese eel (*Anguilla japonica*). *ICES J. Mar. Sci.* **64**, 1387–1395 (2007).
44. Kimura, S., Inoue, T. & Sugimoto, T. Fluctuation in the distribution of low salinity water in the North Equatorial Current and its effect on the larval transport of the Japanese eel. *Fish. Oceanogr.* **10**, 5160 (2001).
45. Kimura, S., Inoue, T. & Sugimoto, T. Fluctuation in the distribution of low salinity water in the North Equatorial Current and its effect on the larval transport of the Japanese eel. *Fish. Oceanogr.* **10**, 5160 (2001).

Figures

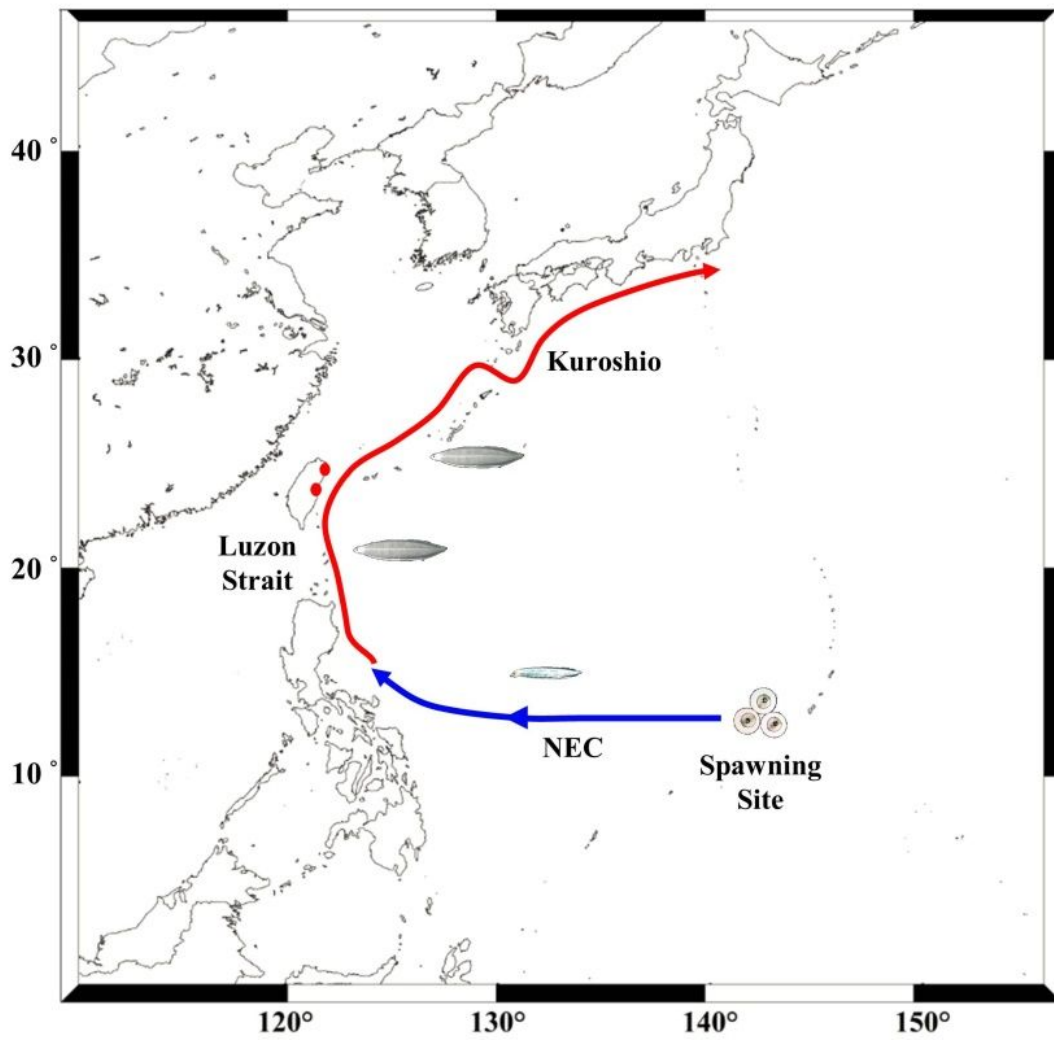


Figure 1

Map showing the spawning site and transport route of the eel larvae to Taiwan and Japan. Red dots indicate the sampling sites of the Japanese glass eel (Yilan and Hualien).

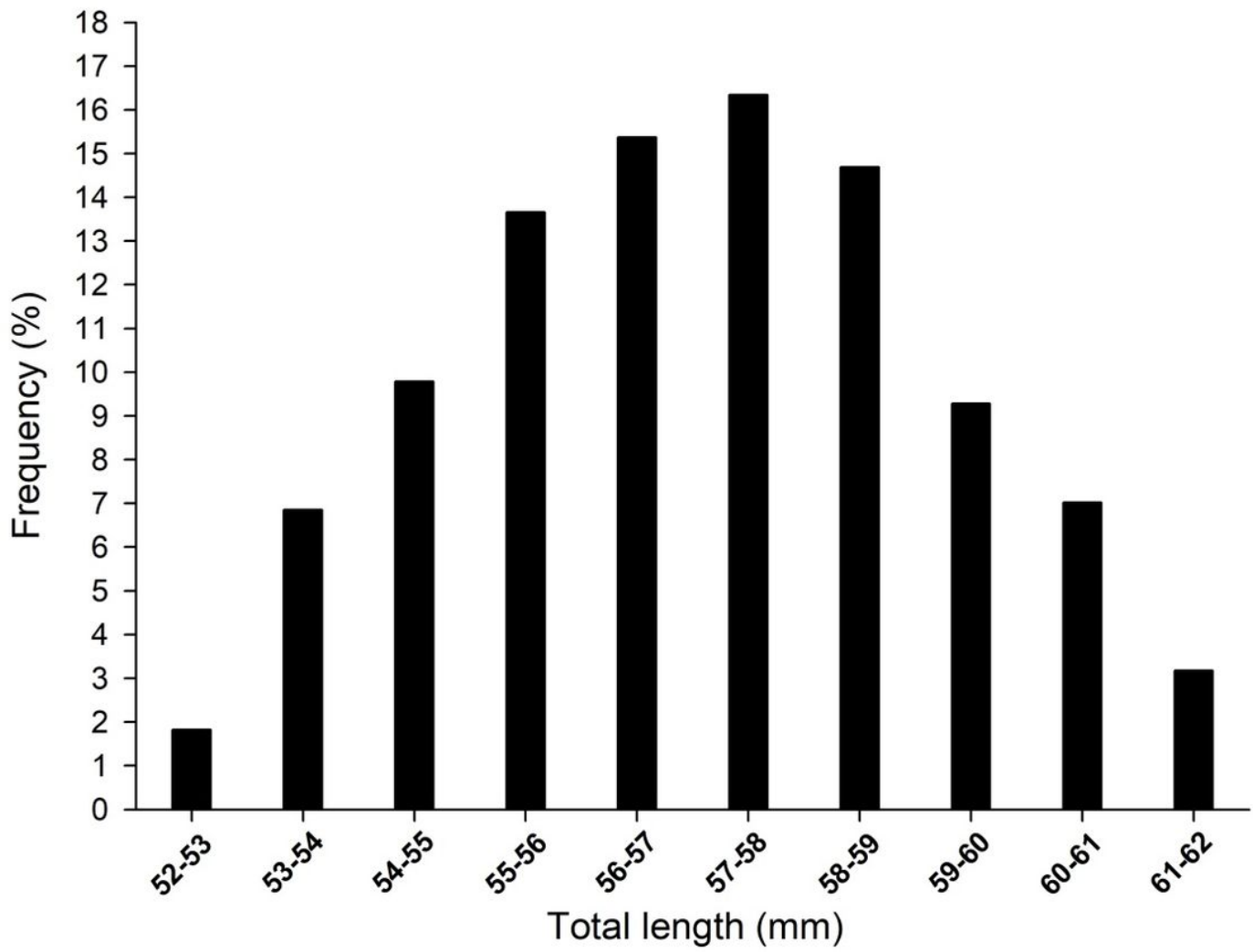


Figure 2

The frequency distribution map of the Japanese glass eel from Taiwan

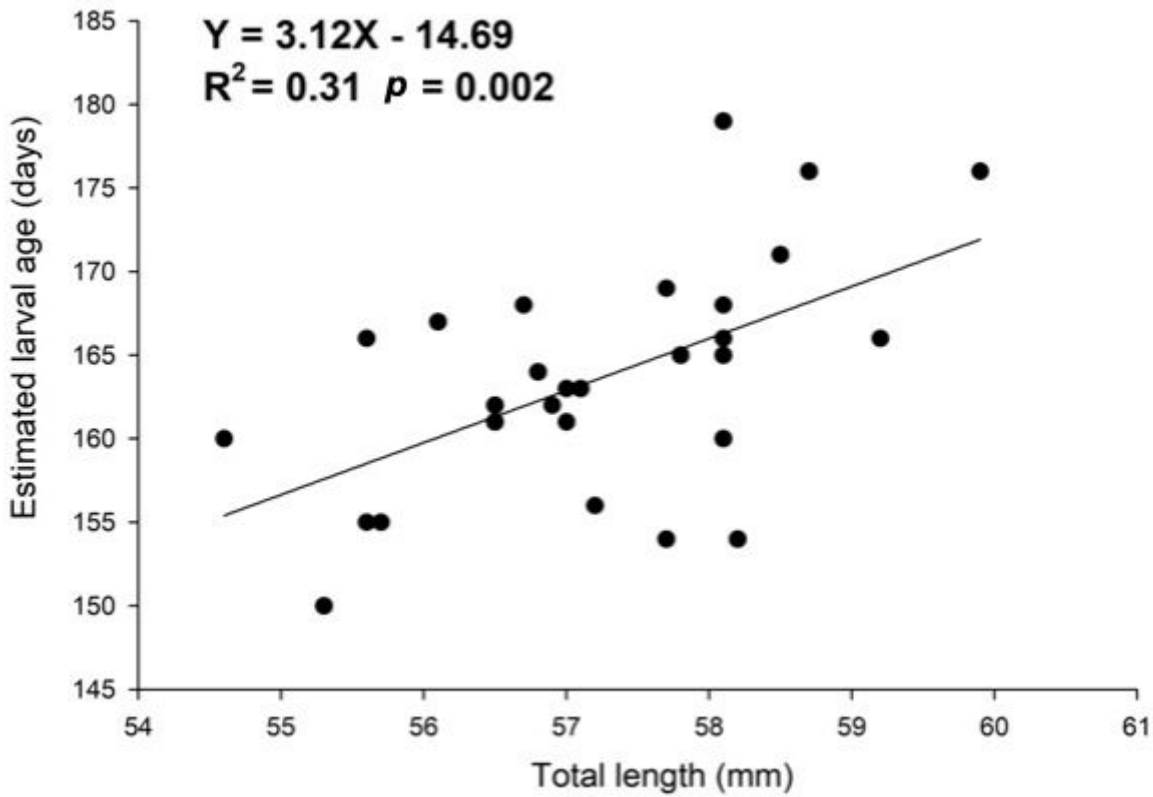


Figure 3

The regression between total length and estimated age of Japanese glass eels transported to eastern Taiwan

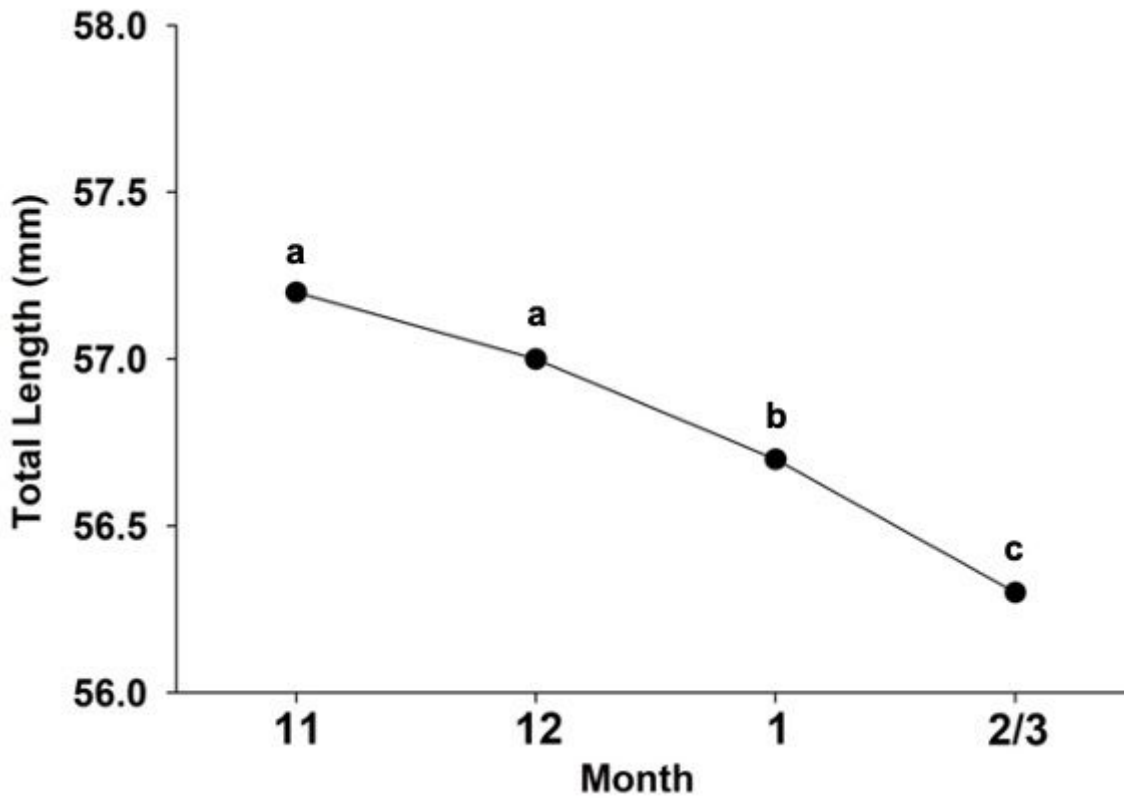


Figure 4

The mean total length of Japanese glass eels from Taiwan (November to February/March)

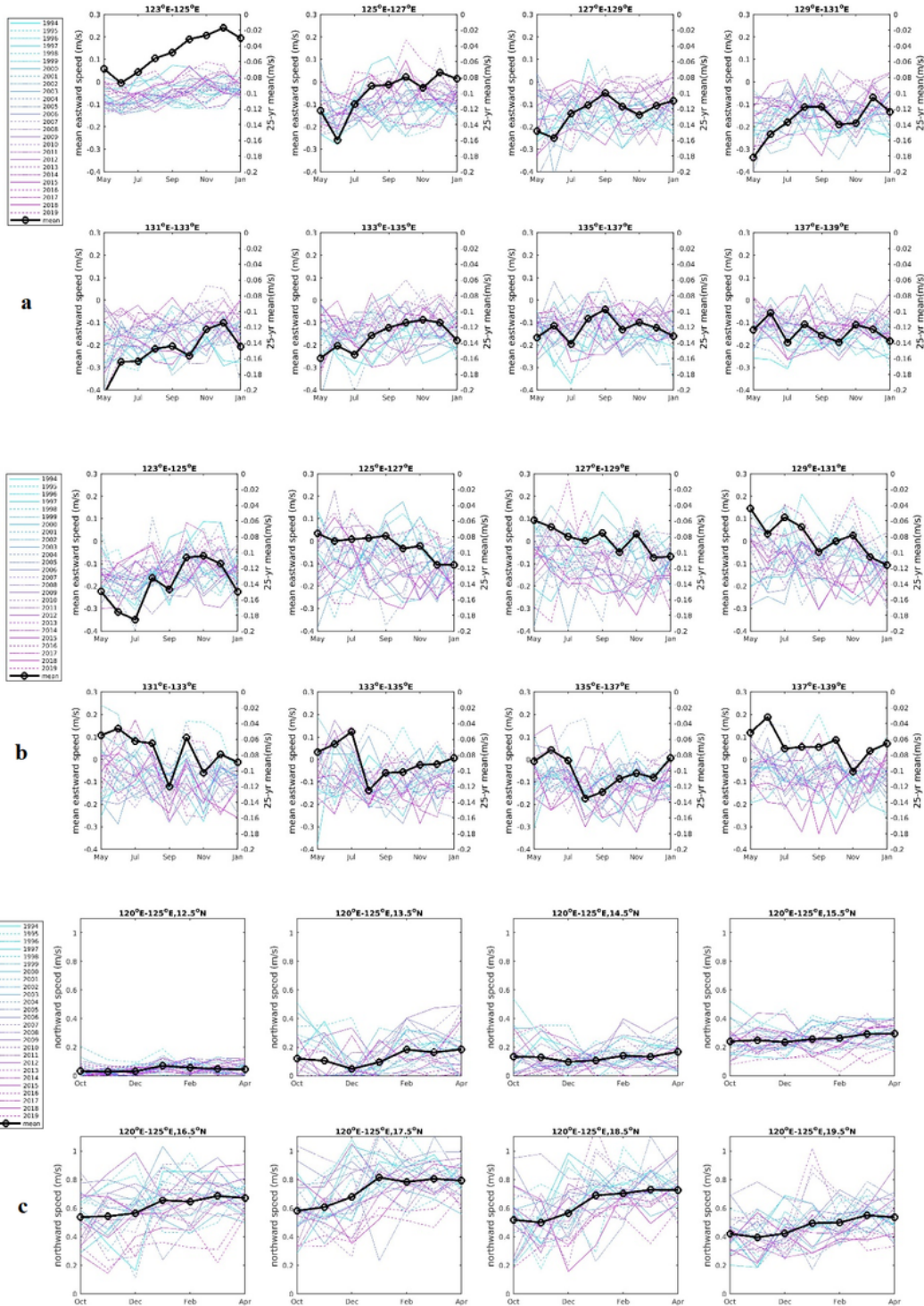


Figure 5

The main stream velocity (m/s, thin lines) of the NEC over 1994–2019 in the region of (a) 13–14° N, (b) 15–16° N and (c) Kuroshio. The 25-monthly mean (1994/5–2019/4) is superimposed (black lines with

circles). The enlarged y-axis at the right shows the trend change.

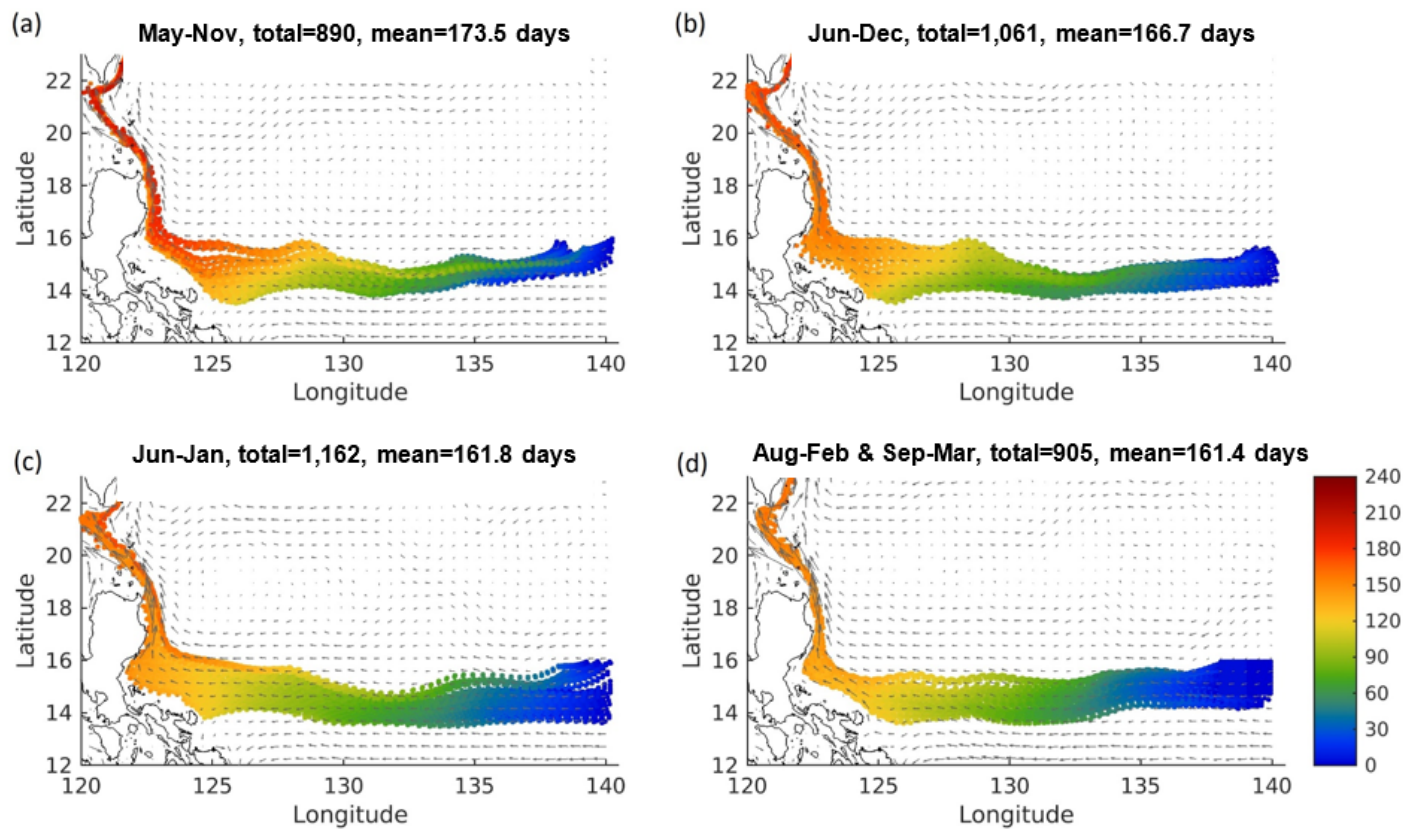


Figure 6

(a) The simulated transport pathways and times (color shaded) of larval Japanese eels from the spawning site (137–140° E, 14–16° N) to Luzon Strait released from May 1st. (b)–(d) released from June 1st, July 1st, and August/September 1st, respectively.

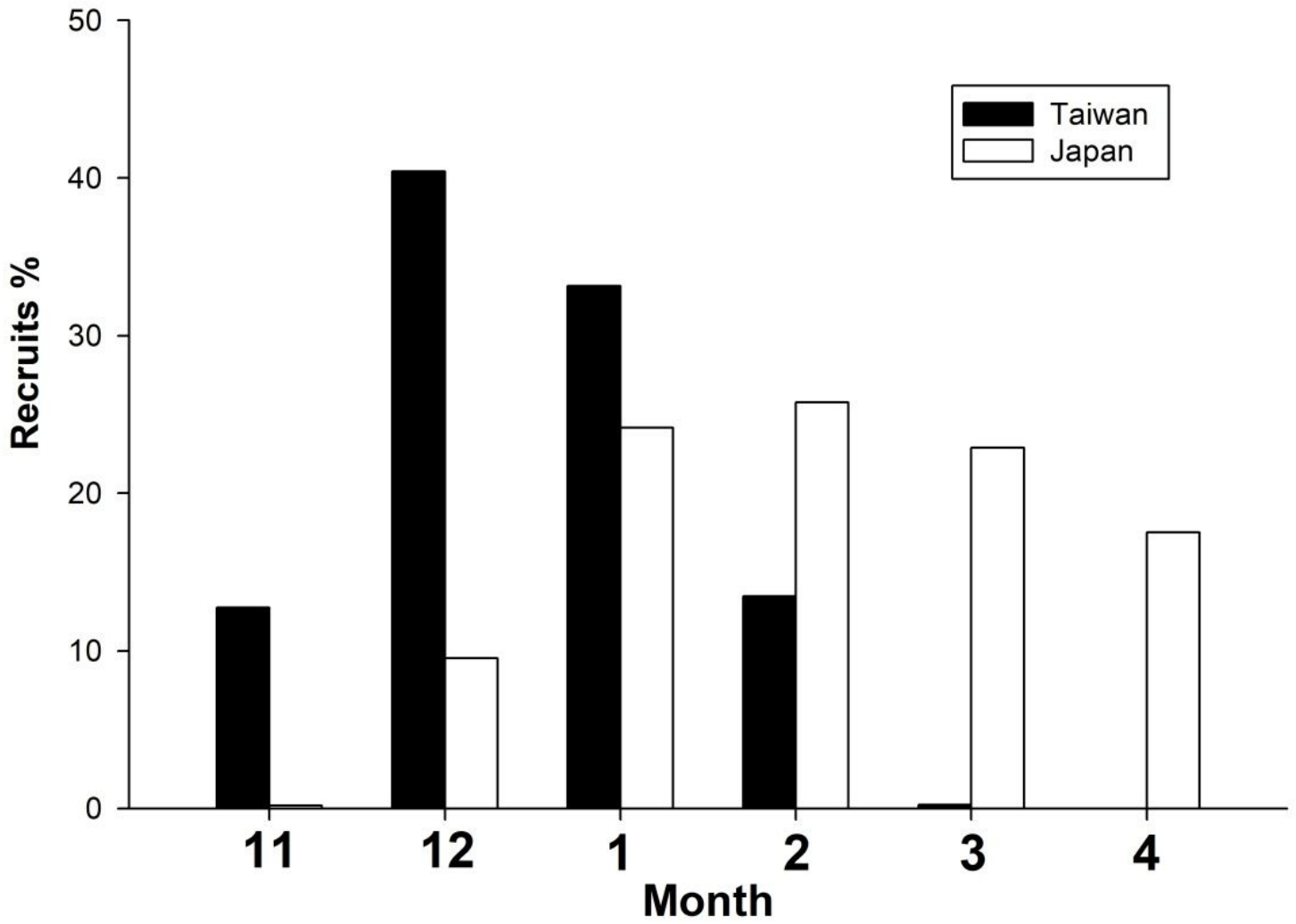


Figure 7

The monthly recruitment percentage of the Japanese glass eel in Taiwan and Japan from November to April

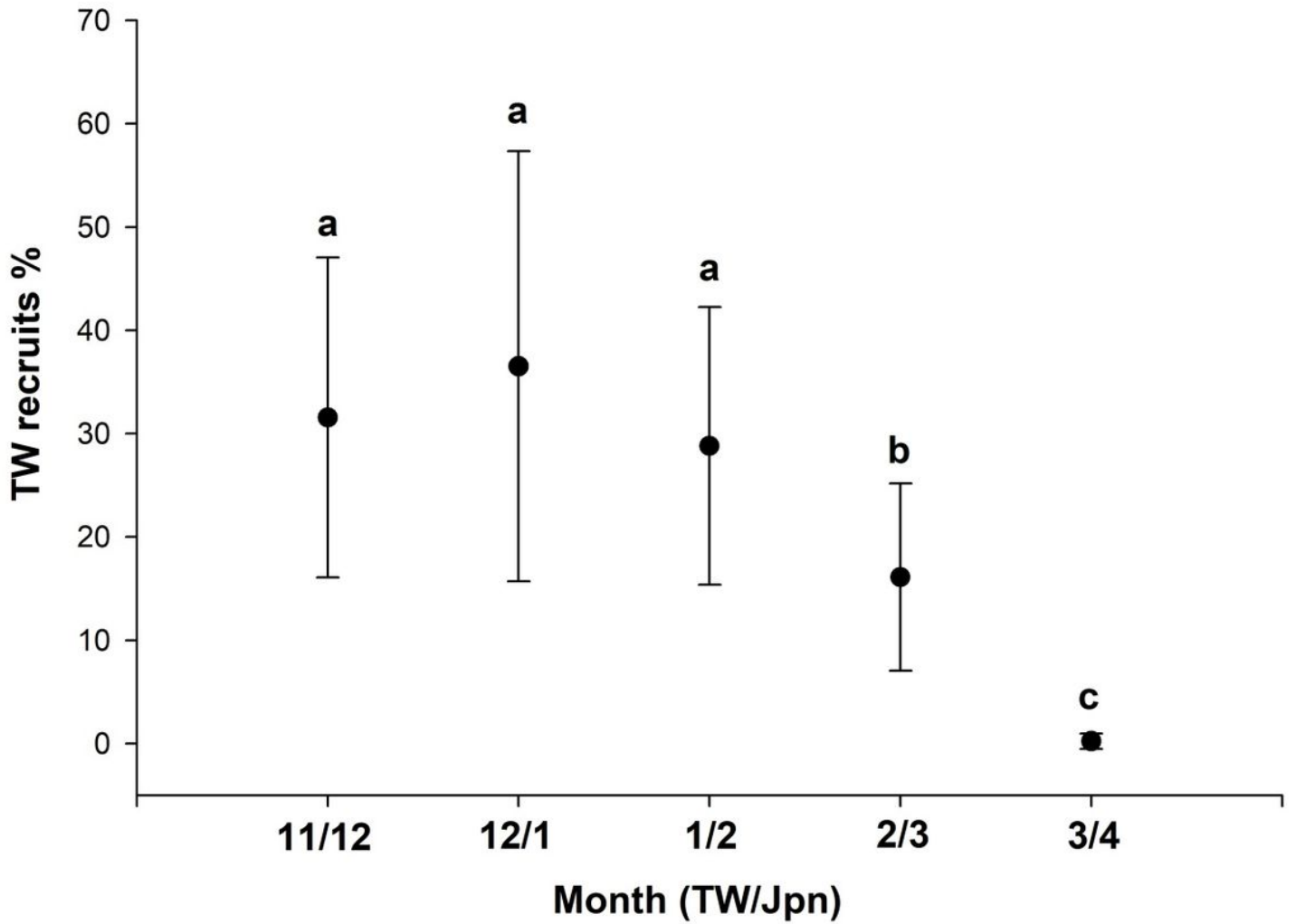


Figure 8

The relative abundance of Japanese glass eels between Taiwan (TW) and Japan (Jpn) from November/December to March/April

Supplementary Files

This is a list of supplementary files associated with this preprint. Click to download.

- [SupplementaryDataset.docx](#)